Multiobjective and robust NVH optimization of automotive ePowertrain including gearbox and emotor excitations

J.-B. Dupont[1], M. Jeannerot[1,2,3], A. Carbonelli[1], S. Lecuru, P. Bouvet[1], E. Sadoulet-Reboul[2], M.Ouisse[2], V.Lanfranchi[3]

1: Vibratec, 28 chemin du Petit Bois, 69130 Ecully, France
2: Univ. Bourgogne Franche Comté, FEMTO-ST Institute, 24 Rue de l'épitaphe, 25000, Besançon, France
3: Université de Technologie de Compiègne, Centre de recherche Royallieu, 60203 Compiègne, France

Abstract: Designing an electrical machine is a complex process that involves many physics, objectives and constraints. Mechanical, thermal and energy performances are usually evaluated and optimized. In order to reach good NVH performance, the acoustic behavior of electrical powertrain has to be considered during the early design phase. Two excitations phenomena are to be considered: electromagnetic excitation within the airgap of the electric motor and meshing processes within the gearbox. The emitted noise is characterized by the emergence of high frequency pure tones that can be annoying and badly perceived by drivers.

For these two sources, the paper will first briefly present efficient computation methods which can be used to estimate noise and vibration levels. For the electromagnetic excitation it relies on a numerical workflow which couples models belonging to the fields of electromagnetics for the Maxwell pressure computations, structural dynamics for the vibration response and acoustics for radiation estimation. For the gearbox excitation, it relies on the computations of excitations terms (Static Transmission Error and mesh stiffness fluctuation) and the spectral iterative solver to obtain the vibration response of the gearbox. Complete powertrain noise computations and examples of validations cases on industrial applications will be shown.

In a second step, the paper will focus on robust optimization methods able to take into account several optimization objectives (sound power, vibration, torque ripple, operating conditions, etc.) and constraints (global efficiency, maximum torque, etc.). In addition to classical deterministic optimization method, robust optimization methods aim at considering the effect of manufacturing tolerances, material properties dispersion and control uncertainties on the vibratory and acoustic levels to minimize, so that noise reduction are really obtained when the machine is manufactured and operated. The interest of robust methods will be illustrated on industrial applications, for electric motor topology optimization as well as gearbox teeth microgeometry optimization.

Keywords: Acoustics, Design Optimization, Electric Motors, Electromagnetics, Robustness, Gearbox, Transmission error, teeth correction.

1. Introduction

Will the advent of electric vehicles force acousticians working in the automotive sector to retire? Most people are convinced that an electric powertrain is necessarily quiet. This is absolutely not the case although it is true that the noise of an electric powertrain is very different from that of a typical ICE. Apart from noises of classical mechanical origin, the noise radiated by an electric powertrain is due to two specific sources: noise due to electromagnetic excitations (related to the electric motor) and gear noise (related to the gearbox directly associated to the electric motor to compose the ePowertrain).

To estimate the NVH performance of an electric motor numerically, methods performing a weak coupling between electromagnetic and dynamic models are frequently applied to diverse motor technologies [1]-[5]. These methods offer good accuracy when compared with measurements [6], and they enable for the estimation of the level of NVH indicators, such as sound power or dynamic forces generated by any design. Some minimization algorithms can be used in order to modify the electric motors design so as to minimize the radiated noise estimated using the multiphysical workflow, while ensuring, by means of optimization constraints, that overall electromechanical performance criteria, such as mean torque, torque ripple or efficiency, are not deteriorated. Using this method, significant noise level reductions can be achieved, owing to the high sensitivity of the electromagnetic excitation harmonic and spatial content to slight design modifications. Such optimization algorithms are used to reduce the noise of electric motors in [7] and [8]. To overcome the generally high number of cost function evaluations required by optimization algorithms, the authors of these articles use fast modelling workflows, i.e. respectively a fully analytical modelling workflow and a surrogate model. In the present paper, in the context of computing power increase, the use of a more accurate finite element electromagnetic model makes it possible to take full advantage of the noise reduction possibilities offered by slight geometric variations. However, the sensitivity of the electromagnetic

excitations can be so high that slight geometric deviations of the magnetic active parts within the manufacturing tolerances can lead to very high variations of the electromagnetic excitations spectral content and thus to the loss of the radiated noise reductions achieved by optimization. For such cases where deterministic optimization is not suited, a robust optimization method is presented. The probabilistic robust optimization methodology has been used for various applications in dynamics [9,10], but it is applied for the first time to the vibroacoustic optimization of electric motors. It ensures, when considering random deviation of the uncertain parameters, to converge towards a design with a low average noise level, and a low variability. After describing the simulation methodology, the deterministic and robust optimization methods are described and applied to minimize the torque ripple of an automotive traction motor.

Geared systems are the seat of vibrations induced by the meshing process. For this reason, a gearbox is an important source of noise and vibration. The gearbox internal sources of excitation are various. The main source corresponds to fluctuation of the static transmission error (STE) of the gear which transmits the drive torque [11]. Static transmission error corresponds to the difference between the actual position of the driven gear and its theoretical one. Apart from the macroscopic parameters such as the size of the gears and their number of teeth, the literature and the tests show that the noise level radiated by a gearbox is strongly dependent on the teeth design, in particular on the microgeometry. Thus, it appears important to optimize the corrections made to the teeth. Insofar as the teeth corrections are of the same order of magnitude as the manufacturing tolerances, it is essential to consider the robustness of the designs.

2. Simulation workflows

2.1 Multiphysical simulation of electric motors noise

The noise generation process for an electric motor is summarized on Fig.1.It can be divided into four steps:

- The supply of the motor by PWM of the voltage leads to the appearance of high order harmonics in the currents.
- These current harmonics, combined with the stator and rotor geometry and with the windings distributions, result in harmonic contributions in the airgap flux density, and as a consequence to dynamic contributions in the radial and tangential Maxwell pressures, which constitute the prevailing electromagnetic excitation in electric motors, as stated in [12].
- The electromagnetic excitations apply to the stator and the rotor cause vibrations, with an amplitude depending on the modal basis and damping of the powertrain structure, and on the amplitude, frequency and spatial distribution of the electromagnetic excitations.
- Depending on the operating deflection shapes and the vibration frequencies, the structure will prove to be more or less prone to radiating noise and to generate and to transmit dynamic forces to the receiving structure.

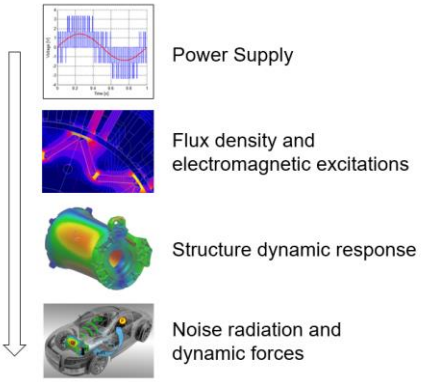

Figure 1: Overview of the noise generation process in electric motors

The numerical simulation of the noise generation process in electric motors requires the modelling of phenomena belonging to different fields of physics. An overview of a 3-steps multiphysical calculation scheme based on finite element models is given on Fig. 2.

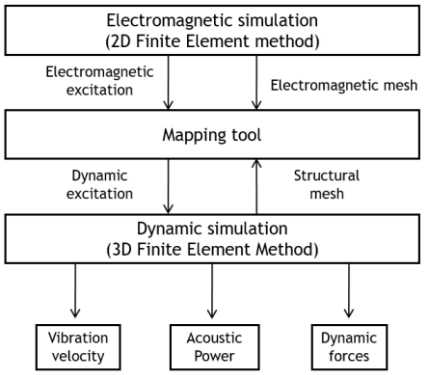

Figure 2: Basic principle of the multiphysical simulation methodology

The motor is first modelled using the electromagnetic 2D finite element method. At this stage, the two first steps of the noise generation process depicted on Fig. 1 are considered, since the supply conditions, the geometric design, the material properties and potential defects such as eccentricity are modelled. From this simulation, the radial and tangential flux densities are calculated along the air gap for different

positions of the rotor. In the examples of the present paper, the motors are fed with sinusoidal currents, but they can equally be fed with current having high order harmonics, following the method presented in [1]. Moreover, the eccentricities are neglected in this paper, but they can be simulated using an electromagnetic finite element model, as performed in [13]. The Maxwell pressures applying to the stator all along the airgap can then be calculated using

$$\sigma_r = \frac{1}{2\mu_0}(B_r^2 - B_t^2), \quad [1]$$

and

$$\sigma_t = \frac{1}{\mu_0}(B_r B_t), \quad [2]$$

where σ is the surface force density, B is the magnetic flux density, μ_0 is the magnetic permeability of vacuum, and r and t denote radial and tangential components.

After converting the Maxwell pressure results from time domain excitations to frequency domain excitations, they are projected onto the structural mesh of the powertrain. This process is performed using a dedicated mapping tool, dealing with the electromagnetic and structural meshes of different sizes and converting the 2D excitations calculated using the electromagnetic simulation into 3D excitations. The principle of the coupling process is explained in [1]. The dynamic response of the structure is then calculated by modal frequency response. The modal basis of the powertrain structure is first extracted, and the dynamic response of each mode under the effect of electromagnetic excitations is calculated. The operating deflection shape is then obtained by summing the contribution of each mode. This simulation workflow based on a coupling between an electromagnetic and a structural model has been used and validated on many practical cases. An example of validation is given in [14]. Some guidelines on the modelling of laminated stators are given in [15].

The last step of the procedure is about the estimation of the NVH indicators. Three of them are commonly used in the automotive industry:

- The vibration velocity or acceleration of the motor's structure.
- The noise radiated by the machine, caused by the interaction of the vibrating structure with the surrounding air (airborne noise).
- The dynamic forces and torque generated by the motor which are responsible for the structure borne noise.

2.2 Gear noise computation

The method for STE calculation retained is classical [16, 17]. Equations describing contact between gears are solved for each meshing position, taking account of the elasto-static deformations and initial gaps between teeth surfaces.

As detailed in [18], STE is considered as the excitation for the dynamic response computation and the noise radiation estimation. This is a rather complex simulation process, but it is not the point of this paper, so it is not detailed here.

2.3 Towards design optimization

Simulation workflows are not a goal, but they are the means to obtain a design that minimizes the noise radiated by the ePowertrain in operating conditions.

These simulation workflows include all the ePowertrain design parameters that are considered relevant. They make it possible to calculate an estimate of the cost function (often the noise radiated by the machine), but also all the characteristic quantities of the operational conditions (values of torques, speed, efficiency, etc.).

Optimization algorithms can therefore be implemented. The objective of these algorithms is to determine the design parameters which make it possible to reduce the cost function (noise or a quantity at the origin of the noise) as much as possible while respecting certain constraints, in particular so as not to reduce the performance of the ePowertrain.

3. Optimization of an automotive ePowertrain

3.1 Presentation of the ePowertrain

The ePowertrain taken as example for this paper is an automotive ePowertrain. It is illustrated by Figure 3.

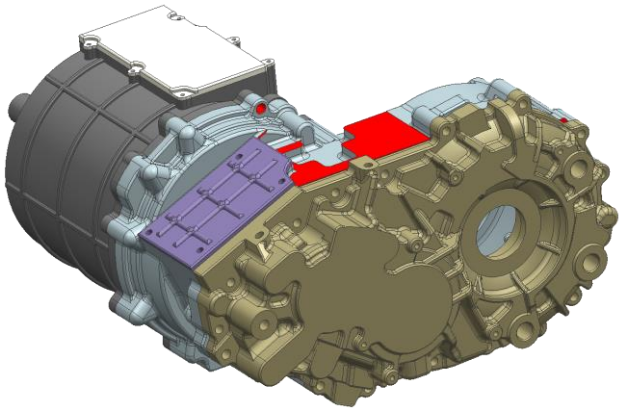

Figure 3: Overview of the ePowertrain

This electric motor is a typical architecture for an automotive electric machine. It is an interior permanent magnets synchronous machine (PMSM) with 8 poles and 48 stator slots. Its rated power is 160kW and the speed range is 0-12000rpm. The motor geometry is illustrated by Figure 4.

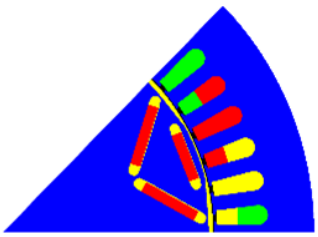

Figure 4: 2D section of the studied motor

The electric motor is associated to a 2-stage gearbox directly flanged on the end bell of the machine. This gearbox has helicoidal gears.

3.2 Electric motor optimization

3.2.1 Initial diagnosis

The interest of analyzing and trying to minimize the vibroacoustic emissions of the considered PMSM was demonstrated by prior experimental investigations on the complete powertrain including the PMSM, the gearbox and the power electronics unit. They are not detailed in this article. They show that high noise levels are reached at low speeds. This is particularly critical because at low motor speeds, electromagnetic noise prevails over aerodynamic and rolling noise in electric vehicles.

Therefore, to identify the causes of the noise emissions, the motor is simulated in the low-speed range from 500 rpm to 3000 rpm, using the simulation workflow detailed in paragraph 2.

After projecting the excitations produced by each rotor part on a structural finite-element model, the phenomenon causing the high noise levels is identified: the noise and vibrations are due to a resonance of an overall powertrain bending mode caused by the torque ripple excitations around this mode's natural frequency, i.e. around 1000 Hz. The shape of this overall bending mode is depicted in Fig.5. As any periodic function, the torque ripple created by the motor can be expressed in the frequency domain using Fourier series decomposition. Engine orders 24, 48 and 96 mainly contribute to torque ripple, and they cause the resonance of the overall bending mode at different engine speeds.

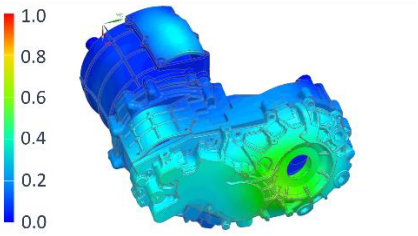

Figure 5: Representation of the powertrain overall bending mode shape (1026 Hz) with unit maximum amplitude color scale.

This resonance, involving an overall powertrain bending mode at 1000 Hz, results in airborne and structure borne noise. The airborne contribution is due to the acoustic radiation of the electric power unit and gearbox cover plates. The dynamic forces resulting from the amplified torque ripple excitation at the attachment points of the motor on the car body are responsible for the structure borne noise.

3.2.2 Deterministic optimization

In order to simplify the simulation process which must be performed for each cost function evaluation required by the optimization, the objective of the optimization is to directly minimize the torque ripple contributions related to engine orders 24, 48 and 96 at the engine speeds at which they reach the frequency of 1000 Hz and provoke the resonance of the overall bending mode, i.e. at 2500 rpm for engine order 24, 1250 rpm for engine order 48 and 625 rpm for engine order 96.

At the same time, attention must as always be paid to the mean torque of the motor so that it is not reduced during the optimization process. This is done by adding an inequality constraint guaranteeing that the mean torque of the optimized design, with no change of the supply currents, remains at the same level as the one of the initial design.

The optimization algorithm that has been implemented is a Sequential Least Squares Programming algorithm (SLSQP). It is an iterative algorithm based on the estimation on the Jacobian matrix. It is compatible with constraints on the optimization parameters as well as on resulting quantities, which is fundamental in our case.

As depicted in Fig. 6, the optimized design produces a much smoother torque.

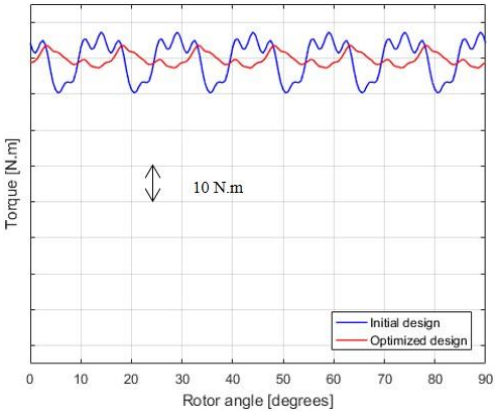

Figure 6: Comparison of the instantaneous torque of the initial and optimized IPMSM at maximum power at 1000 rpm

The torque ripple is significantly reduced for the optimized design, while the mean torque is unchanged. The amplitude reductions of torque engine orders 24, 48 and 96 can be expressed in decibels using

$$R_{DB} = 20\log_{10}\left(\frac{T_{h_{optimized}}}{T_{h_{initial}}}\right), \quad (1)$$

where R_{DB} is the reduction in dB, $T_{h_{optimized}}$ is the amplitude of the hth torque engine order produced by the optimized design and $T_{h_{initial}}$ is the amplitude of the hth torque engine order produced by the initial design.

These torque ripple reductions are summarized in Table 1.

Engine order and critical speed	e.o. 24 at 2500 rpm	e.o. 48 at 1250 rpm	e.o. 96 at 625 rpm
Reduction of the torque harmonics (simulation)	9.1 dB	20.0 dB	11.2 dB

Table 1: Reductions of the numerical torque amplitude levels in comparison with the initial design

As the resonance of the overall bending mode due to torque ripple excitation is prevailing over the other phenomena between 500 and 3000 rpm, expressing the reductions achieved for each torque engine order in dB gives an accurate estimation of the SWL reductions to be expected. As a consequence, the SWL reductions achieved in this case should be close to the torque engine order level reduction values presented in Table 2.

The effect of these modifications on the motor's SWL is calculated using the complete simulation workflow described on Figure 2 and validates the reductions expected when considering torque harmonics. On this basis, a prototype has been built. The experimental results provide the reductions synthetized in Table 2. These reductions of the near field acoustic pressure overall level are even higher than those estimated by the simulations, and they validate the optimization method.

Motor speed	2500 rpm	1250 rpm	625 rpm
Reduction of the near field acoustic pressure (overall level)	11 dB	18 dB	17 dB

Table 2: Reductions of the measured overall acoustic levels in comparison with the initial design.

In this case, the experimental results show that the optimized design is probably robust, although several prototypes should be built or a numerical sensitivity analysis should be conducted to quantify the variability of the optimization cost function when considering geometric deviation.

However, several optimizations starting from different designs have been necessary to reach this optimized design. Many optimizations have converged towards designs achieving very high reductions of the torque engine order 48 level, which reveal to be non-robust minima. Performing robust optimization can ensure the convergence towards a robust minimum.

3.2.3 Robust optimization

The aim of robustness in the case of electric motor acoustics is to minimize the impact of uncertainty sources which cannot be eliminated, i.e. mainly geometry and material properties deviation, as well as control inaccuracies, on the vibratory and acoustic behavior of the motor.

To evaluate the robustness of a given design using this probabilistic approach, the deterministic cost function is expressed in the following way:

$$f = f(x + \delta), \quad (2)$$

where $x = (x_1, \dots, x_N)^T$ is the set of design parameters, which are fixed for the given design, and $\delta = (\delta_1, \dots, \delta_M)^T$ is the set of uncertain parameters, which are considered as random parameters.

A design of given parameters x, and for which all the M uncertain parameters $\delta_i = 0$ are zero, is called nominal design. However, no manufactured design perfectly respects the nominal design because they are all subject to deviations modelled by the uncertain parameters $\delta_i \neq 0$.

In this paper, the assumption is made that the uncertain parameters δ_i follow a normal distribution $\mathcal{N}(0, \sigma_i)$. Their expectation is set to zero, because

systematic deviation can be considered by modifying the nominal design. Their standard deviations σ_i can be estimated from experimental data when measurements are available, or if not, by taking a value of the same order of magnitude as the tolerances, which are usually known.

Some Monte-Carlo samplings are then generated, providing different sets of uncertain parameters δ, and $f(x+\delta)$ is computed for each sample. The mean value μ_f and the standard deviation σ_f of f over all samples are the robustness indicators.

The function to minimize to perform robust optimization is then:

$$\alpha\mu_f + (1-\alpha)\sigma_f, \qquad (3)$$

where $\alpha \in [0,1]$ is a scalar weighting factor defining the trade-off to pursue between mean value and standard deviation minimization. In the rest of the paper, this function is called robust cost function.

The deterministic optimization of the 8-pole PMSM leads to the satisfactory results presented in Table 1 and Table 2. However, many optimizations have been run and some of them have converged towards designs providing very large but also non robust reductions of the torque engine order 48 level. The robustness of one of these non-robust designs is evaluated, and the robust optimization methodology is then applied.

The calculation of the output torque of this skewed PMSM is a relatively long process because of the size of the electromagnetic model and the necessity to model several sections of the motor to account for the skewing effect. This computation time limitation, as well as the fact that the torque engine order 48 is very significantly more variable than the other engine orders when uncertainties are considered, lead to the decision to focus on this engine order 48 at the engine speed of 1250 rpm for this example.

To quantify the robustness of the deterministically optimized non-robust design, the mean value μ_f and standard deviation σ_f of its torque engine order 48 level are calculated with the aid of a Monte-Carlo sampling with 200 samples.

The results of the robustness analysis are presented in Table 3. While the nominal design achieves a reduction of 20 dB in comparison with the initial design, the 200 samples provide a mean reduction of 7.6 dB. Moreover, the high standard deviation means that the torque engine order 48 level, and thus SWL, are very variable, and that while some manufactured motors are significantly less noisy than the initial design, a non-negligible amount of them are as noisy as the initial design or even louder.

e.o. 48 level reduction of nominal design with respect to initial design	e.o. 48 level mean reduction with respect to initial design	e.o. 48 level standard deviation
20.0 dB	7.6 dB	7.0 dB

Table 3: Results of the robustness analysis of the deterministic non-robust design.

The robust optimization methodology presented in this paper can be useful to avoid such non-robust designs and to converge directly towards a robustly silent design. For this purpose, the robust cost function defined in equation (3) is minimized. The weighting factor α is set to 0.5, which means that the same importance is given to the reduction of the mean value and the standard deviation of the torque engine order 48 level. Moreover, an inequality constraint imposing no mean torque reduction must be performed. As the mean torque of the motor is significantly less sensitive to uncertainties than their vibroacoustic behavior, the inequality constraint only guarantees that the nominal optimized design is not subject to any mean torque reduction when compared with the one of the initial design.

The results of this optimization are depicted in Table 5. The design resulting from this optimization provides a much larger mean reduction of the engine order 48 level, with a much lower standard deviation. Both mean value and standard deviation are significantly reduced in comparison with those of the deterministically optimized design which is not robust. The improvement of the robustness is further illustrated by the distributions of the engine order 48 levels reductions for each of the 200 randomly drawn samples of the deterministically and the robustly optimized designs, depicted respectively on Figures 7 and 8.

	e.o. 48 level mean reduction with respect to initial design	e.o. 48 level standard deviation
Deterministically optimized non robust design	7.6 dB	7.0 dB
Robustly optimized design	15.0 dB	2.14 dB

Table 5: Comparison of the robustness analyses of the deterministically optimized non-robust design and the robustly optimized design

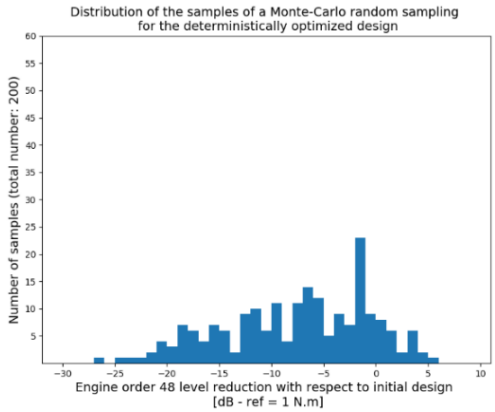

Figure 7: Distribution of the engine order 48 level reduction of the 200 random samples for the deterministically optimized design

Figure 8: Distribution of the engine order 48 level reduction of the 200 random samples for the robustly optimized design

These results show that probabilistic robust optimization can be applied to optimize electric motors when deterministic optimization converges towards non-robust designs. This method has been applied to minimize only the torque engine order 48 at 1250 rpm, because it is the objective which is subject to the highest variability. The robust optimization method being time consuming, because computing the values of μ_f and σ_f, requires several evaluations of the deterministic cost function f, performing a robust multi-objective optimization aiming at minimizing the torque engine orders 24, 48 and 96 at their respective critical engine speeds of 2500 rpm, 1250 rpm and 625 rpm would require a long computation time. An alternative could be to define a multi-objective optimization aiming at minimizing both mean value and standard deviation of the torque engine order 48 at 1250 rpm when uncertainties are considered, and at minimizing the torque engine orders 24 and 96, which are not subject to a high variability when uncertainties are considered, for the nominal design only.

3.2 Gear design optimization

3.2.1 Presentation

The goal of the optimization is to find, for a given initial gear design (i.e. for a given macro geometry), the teeth correction that lead to a minimum sound power radiated by the gearbox integrated inside the ePowertrain in operating conditions.

The value of these teeth corrections are about some micrometers: that is the same order of magnitude as the manufacturing tolerances. Then, it doesn't make any sense to consider a deterministic design optimization: the teeth correction optimization must be robust, or not to be at all.

Since the numerical constraints, in particular, computational time are very different from that of the electric motor, a different optimization algorithm has been chosen for gear design optimization: Particle Swarm Optimization (PSO).

The method is based on a stigmergic behavior of a population, being in constant communication and exchanging information about their location in a given space to determine the best location according to what is being searched (minimizing the STE). In this case, some informant particles are considered, which are located in an initial and random position in a hyper-space built according to the different optimization parameters. The best location researched is thus the combination of parameters which ensures the minimum value of the cost function defined earlier. At each step and for each particle, a new speed and a new position is reevaluated considering the current particle velocity, its current position, its best position, the best position of neighbors.

For complex cases where the computational time for one iteration is low (our case here), this is a very efficient algorithm to reach an optimum. In general, several possible sets of optimized teeth microgeometries are found by the algorithm, as shown in Figure 9.

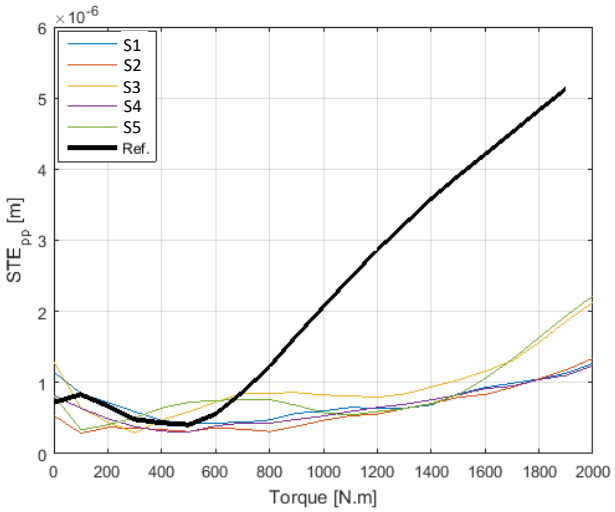

Figure 9: Peak-to-peak value of the STE as a function on the torque.
Before optimization: black curve.
After optimization: colored curves (each color corresponds to a specific optimized teeth microgeometry)

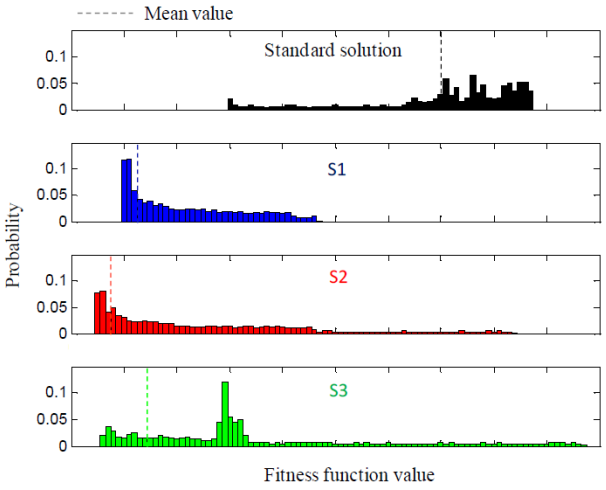

Figure 10: Probability density functions for the standard solution and three selected optimized solutions

3.2.2 Robustness analysis

The selection of the best one(s) is done by means of a robustness analysis considering the sensitivity of the solutions regarding uncertainties due to manufacturing tolerances.

If a solution is determined by the PSO, the robustness can be evaluated by a Monte-Carlo method. Then, 10000 others solutions are computed, chosen randomly in an hyperspace centered on the optimized solution parameters values, limited by the tolerances interval of each parameter and considering possible lead and involute alignment deviations. These 10000 results allow the establishment of the density probability function of each selected optimized solution. They also allow us to compute statistical variables such as mean value and standard deviation.

Figure 10 shows an example of probability density functions for different possible solutions. It illustrates how the optimized solution is selected. The solution S2 has a smaller mean value, but it is associated with a large dispersion. The solution S1 appears to be the best compromise between the mean value and the deterioration capability of the solution.

Conclusion

Electric powertrains that equip new electric vehicles are not so quiet and their design can become a headache for teams dedicated to NVH problems.

The two main sources of noise and vibrations, specific to this type of equipment, are the electromagnetic excitations which apply to the structure of the electric motor and the transmission errors between the gears of the gearbox.

For a complete and successful approach, these two sources must be the object of an optimization procedure. Since the phenomena are very different, they are handled through different simulation workflows. An optimization algorithm is chosen for each of them. Depending on the cases and the dynamic responses that occur under operating conditions, one or the other of these optimizations will lead to the most significant reductions, but it is important to implement the entire optimization process to obtain the best vibroacoustic performance from the initial design.

Acknowledgements

The authors would like to thanks:

- For the work on gears: the LTDS laboratory from the Ecole Centrale of Lyon and the LABCOM Ladage funded by the ANR (National Research Agency).
- For the work on e-motors: the E-Silence project, co-funded by the European Union and the Feder funds in the Auvergne-Rhône-Alpes region.

References

[1] P. Pellerey, V. Lanfranchi and G. Friedrich, “Coupled numerical simulation between electromagnetic and structural models, influence of the supply harmonics for synchronous machine vibrations,” *IEEE Transactions on Magnetics*, vol. 48, no. 2, pp. 983-986, Feb. 2012

[2] A. Tan-Kim, V. Lanfranchi, S. Vivier, J. Legranger and F. Palleschi, “Vibro-Acoustic Simulation and Optimization of a Claw-Pole Alternator,” *IEEE Transactions on Industry Applications*, vol. 52, no. 5, pp. 3878-3885, Sept.-Oct. 2016.

[3] J.-B. Dupont. and H. Saucy, “Noise radiated by electric motors: simulation process and overview of the optimization approaches”, *2017 Automotive Acoustics Conference*, Zurich, Switzerland, pp.107-121.

[4] P. Kotter, D. Morisco, M. Boesing, O. Zirn and K. Wegener, “Noise-Vibration-Harshness-Modeling and Analysis of a Permanent-Magnetic Disc Rotor Axial-Flux Electric Motor,” *IEEE Transactions on Magnetics*, vol. 54, no. 3, pp. 1-4, March 2018.

[5] J. Hallal, A. H. Rasid, F. Druesne and V. Lanfranchi, “Comparison of radial and tangential forces effect on the radial vibrations of synchronous machines,” *2019 IEEE International Conference on Industrial Technology (ICIT)*, Melbourne, Australia, 2019, pp. 243-248.

[6] J.-B. Dupont, P. Bouvet and J.-L. Wojtowicki, “Simulation of the Airborne and Structure-Borne Noise of Electric Powertrain: Validation of the Simulation Methodology,” SAE Technical Paper, 2013.

[7] J. Le Besnerais, V. Lanfranchi, M. Hecquet and P. Brochet, “Multiobjective optimization of induction machines including mixed variables and noise minimization,” *IEEE Transactions on Magnetics*, vol. 44, no. 6, pp. 1102-1105, June 2008.

[8] J. Hallal, P. Pellerey, F. Marion, F. Druesne and V. Lanfranchi, “Harmonic pressure optimization on numerical electric motor model,” *COMPUMAG*, Budapest, Hungary, 2013.

[9] K. H. Hwang, K. W. Lee and G. J. Park, “Robust optimization of an automobile rearview mirror for vibration reduction,” Structural and Multidisciplinary Optimization, no. 21, pp. 300-308, 2001.

[10] C. Zang, M. Friswell, J. Mottershead, “A review of robust optimal design and its application in dynamics,” *Computers and Structures*, no. 83, pp. 315-326, Jan. 2005.

[11] Harris LS (1958) Dynamic loads on the teeth of spur gears. Proc Inst Mech Eng 172:87–112.

[12] J.-B. Dupont, P. Bouvet and L. Humbert, “Vibroacoustic simulation of an electric motor: methodology and focus on the structural FEM representativity,” *2012 XXth International Conference on Electrical Machines*, Marseille, France, 2012.

[13] J.-B. Dupont, R. Aydoun, P. Bouvet, “Simulation of the Noise Radiated by an Automotive Electric Motor: Influence of the Motor Defects,” *International Styrian Noise, Vibration & Harshness Congress*, Graz, Austria, 2014.

[14] J.-B. Dupont, P. Bouvet and J.-L. Wojtowicki, “Simulation of the Airborne and Structure-Borne Noise of Electric Powertrain: Validation of the Simulation Methodology”, *SAE 2013 Noise and Vibration Conference and Exhibition*, Grand Rapids, USA, 2013.

[15] P. Millithaler, E. Sadoulet-Reboul, M. Ouisse, J.-B. Dupont and N. Bouhaddi, “Structural dynamics of electric machine stators: Modelling guidelines and identification of three-dimensional equivalent material properties for multi-layered orthotropic laminates,” *Journal of Sound and Vibration*, vol. 348, pp. 185-205, 2015.

[16] Rigaud E, Barday D (1998) Modeling and analysis of static transmission error of gears: effect of wheel body deformation and interactions between adjacent loaded teeth. Mécanique Industrielle et Matériaux. 51(2):58–60.

[17] Rigaud E, Barday D (1999) Modelling and analysis of static transmission error. Effect of wheel body deformation and interactions between adjacent loaded teeth. In: 4th world congress on gearing and power transmission, Paris, vol 3, pp 1961–1972.

[18] Carbonelli A (2008) Caractérisation vibro-acoustique d’un cascade de distribution poids lourd. Thèse de doctorat de l’Ecole Centrale de Lyon N°2012-34"

Glossary

STE: Static Transmission Error

e.o.: engine order.

IPMSM: Interior Permanent Magnet Synchronous Motor.

PWM: Pulse Width Modulation.

PMSM: Permanent Magnet Synchronous Motor.

SWL: Sound Power Level